

The Influence of Linear Kinematic Hardening and Non-Linear Combined Isotropic-Kinematic Hardening Plasticity Model on Sliding Contact

M. Nagentrau^{1*}, W. A. Siswanto¹ and A. L. Mohd Tobi¹

¹ Faculty of Mechanical and Manufacturing Engineering, Universiti Tun Hussein Onn Malaysia, Batu Pahat, Johor, Malaysia

Abstract— This paper addresses the plastic strain and stress behaviour of sliding contact using two different plasticity models and sliding amplitudes. A numerical two-dimensional (2D) cylinder-on-flat contact model subjected to normal loading and sliding is investigated. The elasto-plastic Ti-6Al-4V alloy is examined under quasi-static condition in this simulation. The influence of Linear Kinematic hardening and Non-Linear Combined Isotropic-Kinematic hardening plasticity models for sliding amplitude of 0.05 mm and 0.2 mm are studied based on plastic strain and stress distributions. Contact pressure, von Mises stress, tangential stress, shear stress, equivalent plastic strain, tangential plastic strain and also shear plastic strain are analyzed on selected specific element from the surface and subsurface of the substrate (flat surface). The FE model is validated and verified with Hertzian contact theoretical solution. The Linear Kinematic hardening plasticity model predicts higher stress response, meanwhile Non-Linear Combined Isotropic-Kinematic hardening plasticity model gives higher plastic strain. The higher sliding amplitude effect results in higher plasticity accumulation.

Index Term— cylinder-on-flat, reciprocating sliding, Ti-6Al-4V, Linear Kinematic hardening, Non-Linear Combined Isotropic-Kinematic hardening

I. INTRODUCTION

Over the past century there has been dramatic increase in the study of contact mechanics as the contact problems are central in solid mechanics. Contact mechanics can be defined as the study of the solid deformation of contacting bodies that touch each other at one or more points [1]. In addition, simulating the contact mechanics by using Hertzian contact condition compromise a challenging yet interesting research subject. Generally,

Hertzian contact theory is applicable with few assumptions such as contacting surfaces are continuous and non-conforming with small strains, frictionless contact and each solid are an elastic half-space [1]. Numerous studies have attempted to explain contact mechanics in elastic regime can be found in the literature [1-4]. Finite element approach in solving complex contact mechanics problem is costly and time consuming. Obviously, appropriate constitutive model must be employed in order to represent behaviour of contacting surface using numerical simulations [5, 6].

Based on physics, plasticity is the tendency of a material to experience a non-reversible and permanent deformation under applied force. Lal and reddy discovered that it is mandatory to study the material behaviour at the atomic scale in order to study the plastic deformation [7]. Kachanov raised several concerns about plastic properties where it depends on materials and also ambient conditions [8]. More recent study of Mohd Tobi et al. proves that plastic deformation is one of the major factor that leads to wear in material [9]. Finite element result demonstrated by Mohd Tobi et al. for gross sliding conditions promotes plastic shearing across a wide region that leads to the plastic deformation and accumulation of plastic strain and end up in wear debris generation and delamination cracking [9]. The elastic plastic stress strain response plays a pivotal role in the design and failure analyses of engineering components [10]. For the isotropic hardening, if a solid is deform plastically, and then unload it and reload it again, the yield stress or elastic limit would have increase compare to what it was in the first cycle. If the step is repeated again, the yield stress or the elastic limit will increase further.

M. Nagentrau is a research assistant in Faculty of Mechanical and Manufacturing Engineering, Universiti Tun Hussein Onn Malaysia (phone: +600174039241; fax: 60074536080; e-mail: nagentrau.rau17@yahoo.com).

W. A. Siswanto, is an Associate Professor in Faculty of Mechanical and Manufacturing Engineering, Universiti Tun Hussein Onn Malaysia (e-mail: waluyo@uthm.edu.my).

A. L. Mohd Tobi is a senior lecturer Faculty of Mechanical and Manufacturing Engineering, Universiti Tun Hussein Onn Malaysia (e-mail: abdlatif@uthm.edu.my).

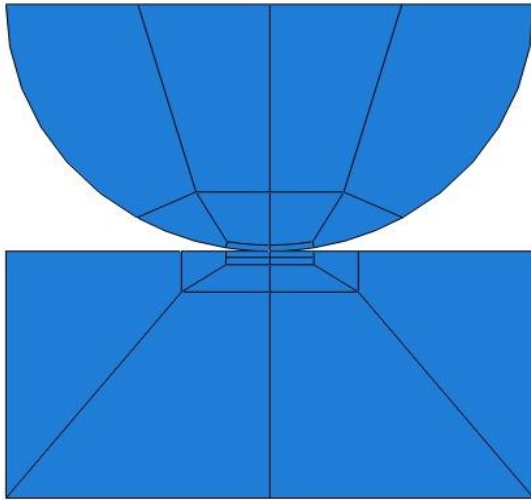


Fig. 1. Partitioned 2D Finite Element geometry.

The evolution law of this model consists of a linear kinematic hardening component that describes the translation of the yield surface in stress space through the back stress. In combined hardening, it consists of two components which are nonlinear kinematic hardening component and an isotropic hardening component. The nonlinear kinematic hardening component describes the translation of the yield surface in stress space through the back stress. The isotropic hardening component describes the changes of the equivalent stress defining the size of the yield surface as a function of plastic deformation [11].

In this paper, the plastic strain and stress behaviour of reciprocating sliding contact using two different plasticity models and sliding amplitudes is studied. The maximum contact pressure and contact half-width length of FE model is verified with Hertzian contact theoretical solution for validation purpose. The predicted plastic strain along with stress distributions for both plasticity hardenings are compared and discussed.

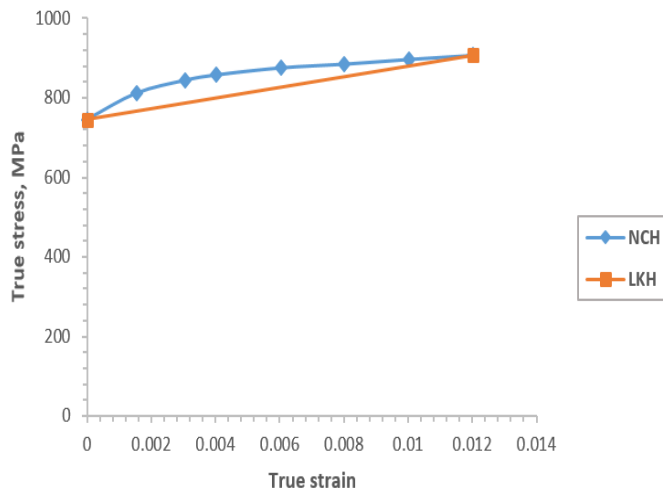


Fig. 2. Plastic stress-strain curves [13]

II. FE MODELLING APPROACH

A commercial Finite Element software ABAQUS/Standard is

TABLE I
PLASTICITY HARDENING AND SLIDING AMPLITUDE CASES

Plasticity Hardening	Sliding amplitude
Linear Kinematic Hardening (LKH)	0.05 mm
	0.2 mm
Non-Linear Combined Isotropic-Kinematic hardening (NCH)	0.05 mm
	0.2 mm

practiced to model the reciprocating sliding contact using two different plasticity models and sliding amplitudes under quasi-static condition. A cylinder-on-flat contact configuration model is employed throughout this study [12]. A corresponding two dimensional (2D) finite element model consist of half circle as the indenter with the radius of 6 mm and a rectangle as substrate with the dimension of 12 mm x 6 mm is employed as shown in Fig. 1.

Light weight alloy Ti-6Al-4V which is an aeroengine specific material is examined in this numerical study. The Young's modulus, E of 115 GPa and Poisson's ratio, ν of 0.3 are assigned for Ti-6Al-4V material [9, 12]. Two types of plastic model are examined in this study, i.e. Linear Kinematic hardening (LKH) and Non-Linear Combined Isotropic-Kinematic hardening (NCH). The plasticity data for both hardening models are obtained from the study presented by Benedetti and Fontanari [13]. In addition, the plasticity data for Linear Kinematic hardening (LKH) and Non-Linear Combined Isotropic-Kinematic hardening (NCH) is illustrated in Fig. 2. The linear quadrilateral plane strain elements which are suitable for friction involved contact cases [11] are used throughout this simulation for both plasticity hardening models. Refined mesh with the size of 50 μm is used at

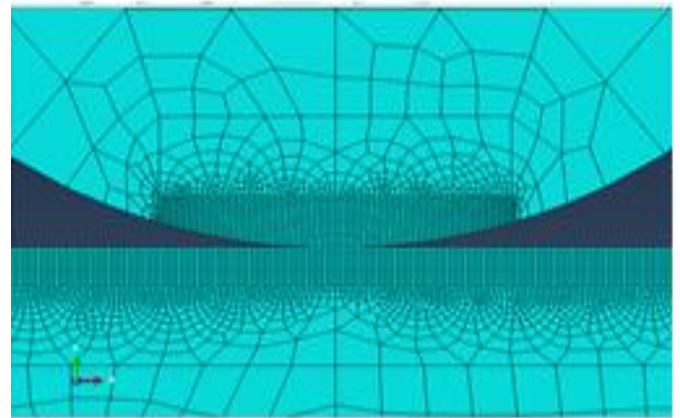


Fig. 3. Mesh module of the 2D contact model

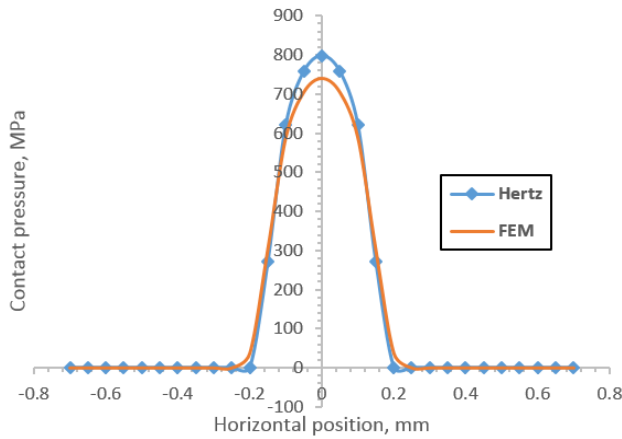


Fig. 4. Contact pressure and contact half-width length comparison between FEM simulation and Hertzian contact theoretical solution for Ti-6Al-4V.

contact region and mesh transition from coarse to fine is achieved via edge seeding approach as shown in Fig. 3. Mesh refinement at contact region is practiced in order to get better prediction of plastic strain and stress distributions with reasonable computational time. Surface-to-surface contact approach is used by introducing two types of contact pairs such as master and slave surfaces. The half cylinder (indenter) acts as master surface meanwhile, the flat surface (substrate) is employed as slave surface. The Lagrange multiplier contact formulation with friction coefficient, μ of 0.9 is utilised to ensure exact stick condition without any slip based on Coulomb friction. Three element sets such Point load, Top and Bottom surfaces is assigned to assist in applying the parameters.

The substrate's bottom surface is constrained from any translation and rotation motions using ENCASTRE boundary condition throughout the simulation. The simulation is performed with two steps, i.e. loading and sliding. The static general step with the step time of 1 s and maximum of 100 increments is assigned. A concentrated normal load, P of 200 N is applied at the Point load during loading step. For sliding step, the displacement amplitude, δ of 0.05 mm and 0.2 mm are applied for case 1 and case 2 respectively as shown in Table 1. The Equation's type constraint is used to ensure the

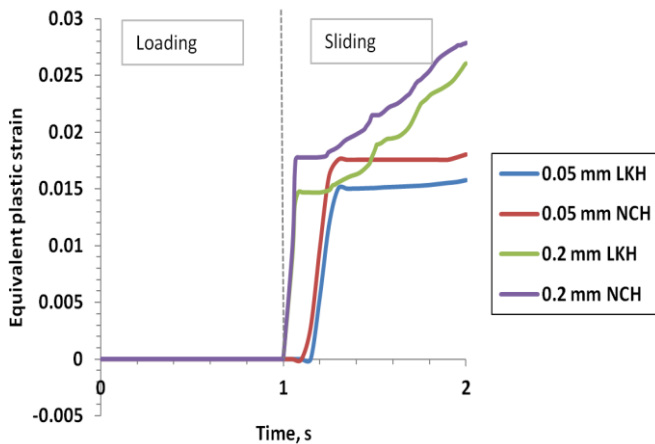


Fig. 5. The equivalent plastic strain history for LKH and NCH.

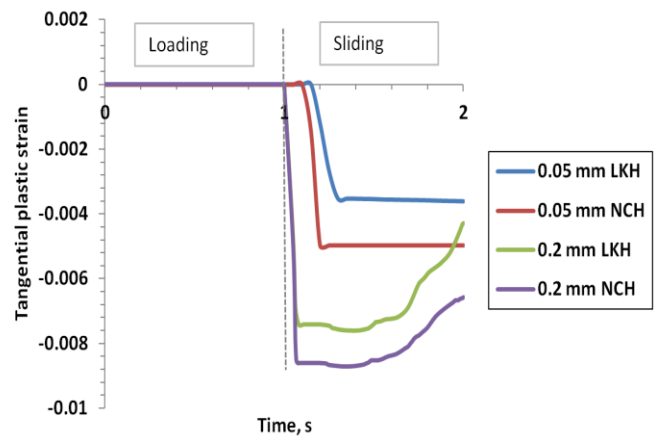


Fig. 6. The tangential plastic strain history for LKH and NCH

whole indenter translate concurrently with the Point Load. The FE analysis is carried out for both plasticity hardening model to study the plastic strain and stress distributions. The FE model is validated and verified using Hertzian theoretical solution.

III. RESULTS AND DISCUSSION

The findings of present study revealed that the influence of different plasticity hardening and sliding amplitude on plastic strain and stress distributions using numerical approach. Ti-6Al-4V alloy contact condition is examined. The contact pressure distributions obtained from the surface of the substrate by creating a path line, meanwhile, plastic strain and stress distributions are taken from the specific element where maximum plastic strain and stress occur.

A. FE Model Verification

Fig. 4 illustrates comparison of theoretical and numerical contact pressure distributions. The FE predicted contact

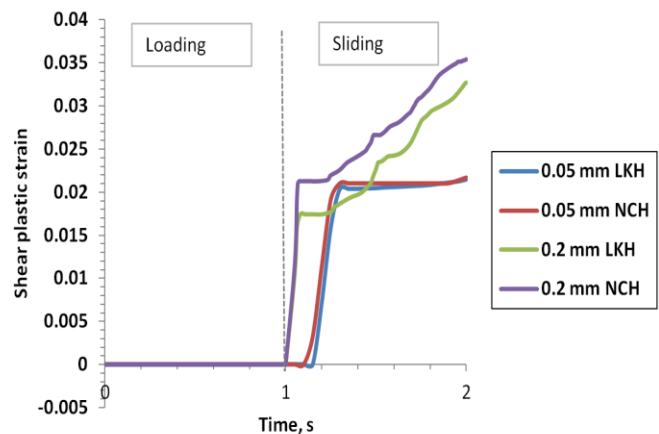


Fig. 7. The shear plastic strain history for LKH and NCH

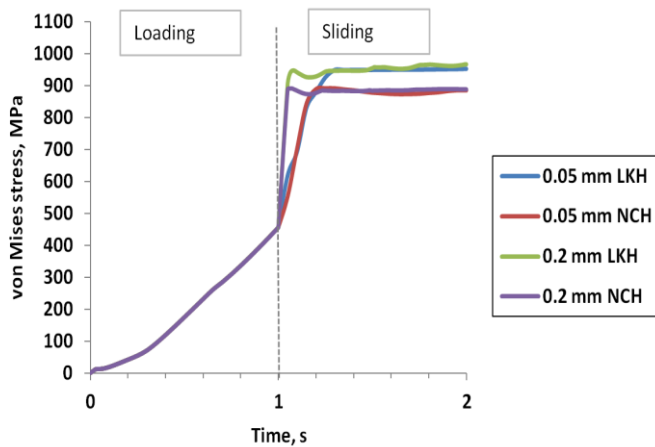


Fig. 8. The von Mises stress history for LKH and NCH

pressure distribution shows similar trend as Hertzian contact theoretical solutions where the maximum contact pressure occurs at the centre of the contact. The calculated maximum contact pressure, p_0 and contact half-width length, a are 798.6 MPa and 0.2 mm respectively. Meanwhile, the FE predicted maximum contact pressure, p_0 and half-width contact length, a are 740.9 MPa and 0.3 mm. The FE predicted contact distribution gives good agreement with Hertzian theoretical solution.

B. Equivalent Plastic Strain Evolution

Fig. 5 illustrates equivalent plastic strain history of different plasticity hardening and sliding amplitude for Ti-6Al-4V material. The trend of the graph shows that the equivalent plastic strain is not significant for all the cases during loading step. The equivalent plastic strain started to increase rapidly during early stage of sliding step. It is apparent that higher sliding amplitude (0.2 mm) records higher equivalent plastic strain compared with lower sliding amplitude (0.05 mm). The most striking results to emerge from the data is that, the material with Non-Linear Combined Isotropic-Kinematic hardening (NCH) has significant equivalent plastic strain value compared with Linear Kinematic hardening (LKH) for both sliding amplitudes. The maximum equivalent plastic strain recorded for the LKH with 0.05 mm sliding amplitude, LKH with 0.2 mm sliding amplitude, NCH with 0.05 mm sliding amplitude, NCH with 0.2 mm sliding amplitude are 0.016, 0.027, 0.018 and 0.028 respectively.

C. Tangential Plastic Strain Evolution

Fig. 6 presents tangential plastic strain history of different plasticity hardening and sliding amplitude for Ti-6Al-4V material. The trend of the graph indicates that the tangential plastic strain is not significant for all the cases during loading step. The tangential plastic strain started to increase in negative manner during early stage of sliding step. The maximum tangential plastic strain for lower sliding amplitude maintains the maximum value until end of the sliding step, meanwhile for higher sliding amplitude case the tangential

plastic strain drops slowly after achieving the maximum value.

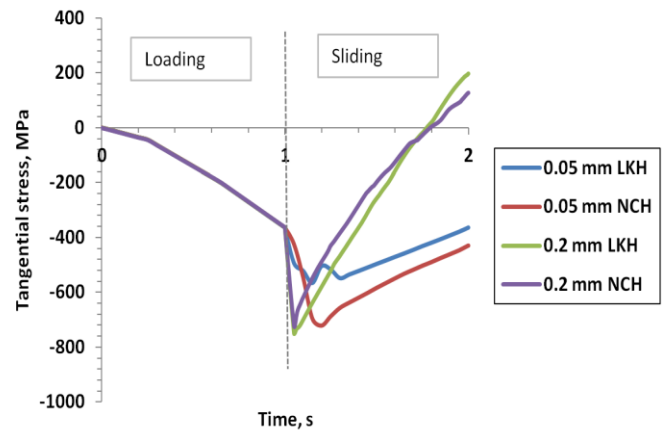


Fig. 9. The tangential stress history for LKH and NCH

It is obvious that higher sliding amplitude (0.2 mm) records higher equivalent plastic strain compared with lower sliding amplitude (0.05 mm). The present finding also consistent with the equivalent plastic strain where the material with Non-Linear Combined Isotropic-Kinematic hardening (NCH) exhibits higher tangential plastic strain value compared with Linear Kinematic hardening (LKH) for both sliding amplitudes. The maximum tangential plastic strain recorded for the LKH with 0.05 mm sliding amplitude, LKH with 0.2 mm sliding amplitude, NCH with 0.05 mm sliding amplitude, NCH with 0.2 mm sliding amplitude are 0.004, 0.008, 0.005 and 0.009 correspondingly.

D. Shear Plastic Strain Evolution

Fig. 7 is the shear plastic strain history of different plasticity hardening and sliding amplitude for Ti-6Al-4V material. The trend of the graph reveals that shear plastic strain is not noteworthy for all the cases during loading step. The shear plastic strain started to rise rapidly during early stage of sliding step. It is noticeable that higher shear plastic strain is recorded for higher sliding amplitude (0.2 mm) records compared with lower sliding amplitude (0.05 mm). The results indicate that Ti-6Al-4V material with Non-Linear Combined Isotropic-Kinematic hardening (NCH) displays higher shear plastic strain value compared with Linear Kinematic hardening (LKH) for both sliding amplitudes. The maximum shear plastic strain recorded for the LKH with 0.05 mm sliding amplitude, LKH with 0.2 mm sliding amplitude, NCH with 0.05 mm sliding amplitude, NCH with 0.2 mm sliding amplitude are 0.0214, 0.0327, 0.0217 and 0.0354 respectively.

E. Von Mises Stress Evolution

Fig. 8 shows the von Mises stress history of different plasticity hardening and sliding amplitude for Ti-6Al-4V material. The trend of the graph reveals that von Mises stress increasing simultaneously for all the cases during loading step. The difference in von Mises stress noticeable during sliding step according to each condition. Higher von Mises stress is recorded for Linear Kinematic hardening (LKH)

compared with Non-Linear Combined Isotropic-Kinematic

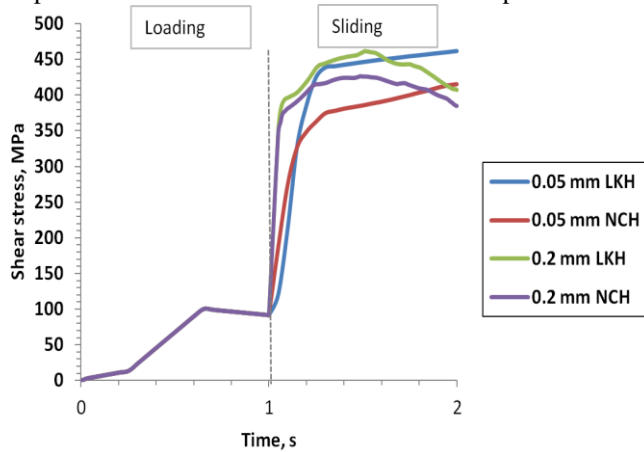


Fig. 10. The shear stress history for LKH and NCH

hardening (NCH) for both sliding amplitudes. The results also signify that the effect of plasticity hardening is more noticeable compared with sliding amplitudes where only small changes in von Mises stress is observed when alter the sliding amplitudes on Ti-6Al-4V contact pairs. The maximum von Mises stress recorded for the LKH with 0.05 mm sliding amplitude, LKH with 0.2 mm sliding amplitude, NCH with 0.05 mm sliding amplitude, NCH with 0.2 mm sliding amplitude are 953.24 MPa, 966.54 MPa, 891.75MPa and 891.80 MPa respectively.

F. Tangential Stress Evolution

Fig. 9 illustrates tangential stress history of different plasticity hardening and sliding amplitude for Ti-6Al-4V material. The tangential plastic stress in started to increase in negative manner during stage of loading step. The trend of the graph displays that maximum tangential stress recorded during early stage of the sliding and followed by dropping slowly until the end of the particular step. In addition, higher sliding amplitude (0.2 mm) case exhibits higher gradient graph compared with lower sliding amplitude (0.05 mm). The current result also consistent with the von Mises stress where the material with Non-Linear Combined Isotropic-Kinematic hardening (NCH) exhibits lower tangential stress value compared with Linear Kinematic hardening (LKH) for both sliding amplitudes at end of sliding step. The maximum tangential stress recorded for the LKH with 0.05 mm sliding amplitude, LKH with 0.2 mm sliding amplitude, NCH with 0.05 mm sliding amplitude, NCH with 0.2 mm sliding amplitude are -564.82 MPa, -749.73 MPa, -722.24 MPa and -723.69 MPa correspondingly.

G. Shear Stress Evolution

Fig. 10 exhibits the shear stress history of different plasticity hardening and sliding amplitude for Ti-6Al-4V material. The trend of the graph reveals that stress is rising slowly during loading step. The shear stress is significant during stage of sliding step. It is noticeable that shear stress drops after reaching maximum stress for higher sliding amplitude (0.2 mm), meanwhile lower sliding amplitude (0.05 mm) reach

maximum and maintains the value. The results also indicate that Ti-6Al-4V material with Non-Linear Combined Isotropic-Kinematic hardening (NCH) displays lower shear stress compared with Linear Kinematic hardening (LKH) for both sliding amplitudes. The maximum shear plastic strain stress recorded for the LKH with 0.05 mm sliding amplitude, LKH with 0.2 mm sliding amplitude, NCH with 0.05 mm sliding amplitude, NCH with 0.2 mm sliding amplitude are 461.43 MPa, 461.458 MPa, 415.22 MPa and 426.46 MPa respectively.

H. Discussion

Obviously, the contact pressure distribution is mainly depending on the normal load. In addition, the contact pressure distributions and contact half-width length for FE simulation show slight difference when compared with theoretical solution due to the elastic half-space assumption in theoretical solution, whereas not the case for numerical model. The equivalent plastic strain recorded is greater for higher sliding amplitudes due to high surface traction. Besides that, the equivalent plastic strain for Non-Linear Combined Isotropic-Kinematic hardening (NCH) is higher compared with Linear Kinematic Hardening (LKH) as LKH is hardened and does not show any increment in strain, meanwhile NCH exhibits real material characteristics where equivalent plastic strain slightly higher. In addition, when NCH is practiced, the yield surface range may expand or contract due to the isotropic component. This feature allow modelling of inelastic deformation in metals that are subjected to normal and tangential loading. The tangential plastic strain showing same trend as the equivalent plastic strain where higher sliding amplitude and NCH present higher tangential plastic strain. This is mainly due to higher sliding causes strain to material due to surface traction. As the data extracted from only one specific element, the value tend to reduce after reach the maximum tangential plastic strain, especially at higher sliding amplitude. Based on the strain results, the shear plastic strain is much more significant than the tangential plastic strain as the sliding process causes this phenomenon. In addition, both plasticity models exhibits the Bauschinger effect where the effect is usually related to the yield strength of the metal that decreases with the direction of strain changes. To determine which model is much more accurate, the LKH model is just a simple model that gives only a first approximation of the metals behaviour subjected to normal and tangential loading, meanwhile the NCH model which exhibits the real material behaviour by displaying both isotropic and kinematic hardenings can provide more convincing results in many cases. Meanwhile, for the von Mises stress, the LKH model records higher stress compared with NCH. In addition, the sliding amplitude does not really affect the stress where the variation in stress significant due to different in plasticity hardenings. This situation occurs as isotropic hardening displays saturated stress while kinematic hardening shows the stress which is not saturated and keeps on increasing as the strain increasing. However, the effect of sliding amplitude is visible in tangential stress graph as tangential component mainly depend on the displacement of the contact material in x-axis.

This research can contribute on selecting appropriate plasticity model for elastic-plastic finite element approach which can represent the essential features of the physical problem, especially using Ti-6Al-4V material [14, 15]. In addition, elastic-plastic finite element modelling related to the nonlinear industrial applications such as aeroengine sector can promise better plasticity prediction with the appropriate plasticity model which exhibits the real material behaviour of Ti-6Al-4V material.

IV. CONCLUSION

The main objective of the current study is to investigate the influence of different plasticity hardenings and sliding amplitude on the plastic strain and stress distributions for Ti-6Al-4V material using cylinder-on-flat contact configuration FE model. The FE model gives a better agreement with Hertzian maximum contact pressure and contact half width length. It is found that, the Linear Kinematic hardening (LKH) plasticity model predicts higher stress response, meanwhile Non-Linear Combined Isotropic-Kinematic hardening (NCH) plasticity model gives higher plastic strain. The average maximum equivalent plastic strain recorded for LKH is 0.021, meanwhile 0.023 for NCH. Besides that, the average maximum von Mises stress recorded are 959.89 MPa and 891.78 MPa for LKH and NCH respectively. Besides that, the higher sliding amplitude effect results in higher plasticity accumulation.

ACKNOWLEDGMENT

The authors acknowledge the financial support by the Ministry of Education Malaysia and Centre for Graduate Studies (CGS) Universiti Tun Hussein Onn Malaysia. This research is supported by the Research Acculturation Collaborative Effort (RACE), Vot. No. 1441.

REFERENCES

- [1] K. L. Johnson, "Contact Mechanics", Cambridge University Press, Cambridge, 1985.
- [2] S. P. Timoshenko and J. N. Goodier, "Theory of elasticity", *International Journal of Bulk Solids Storage in Silos*, 1(4), 2014.
- [3] N. Kikuchi and J. T. Oden "Contact problems in elasticity: A study of variational inequalities and finite element methods", SIAM Stud Appl Math, 1988.
- [4] R. Hill, "Theoretical plasticity of textured aggregates", *Mathematical Proceedings of the Cambridge Philosophical Society* (Vol. 85, No. 01, pp. 179-191). Cambridge University Press, 1979.
- [5] V. Ciampi and M. A. Crisfield "Non-linear Finite Element Analysis of Solids and Structures", *Meccanica*, 32(6), 586-587, 1997.
- [6] E. A. De Souza Neto, D. Peric and D. R. J. Owen "Computational methods for plasticity: theory and applications", John Wiley & Sons, 2011.
- [7] G. K. Lal, and N. V.Reddy, "Introduction to Engineering Plasticity", Alpha Science International Limited, 2009.
- [8] L. M. Kachanov, "Fundamental of theory of plasticity". Amsterdam, north-Holland Pub Co., 1971, in series: North-Holland series in applied mathematics and mechanic ISBN 0-486-43583-0, 2004.
- [9] A. L. Mohd Tobi, J. Ding, G. Bandak, S. B. Leen and P. H. Shipway, "A study on the interaction between fretting wear and cyclic plasticity for Ti-6Al-4V. *Wear*, 267 pp. 270-282, 2009.

- [10] Y. Jiang and J. Zhang, "Benchmark experiments and characteristic cyclic plasticity deformation", *International Journal of Plasticity*, 24(9), 1481-1515, 2008.
- [11] Dassault Systemes, "Abaqus Theory Manual", Version 6.10. RI, USA, 2010.
- [12] M. Nagentrau, W. A. Siswanto and A. L. Mohd Tobi, "Investigation on the effect of linear kinematic hardening model on plasticity prediction of reciprocating sliding contact", *Applied Mechanics and Materials*, 773-774 (2015) 183-187, 2015.
- [13] M. Benedetti and V. Fontanari, "The effect of bi-modal and lamellar microstructure of Ti-6Al-4V on the behaviour of fatigue cracks emanating from edge notches", *Fatigue Fracture of Engineering Materials Structures* 27 (11) 1073-1089, 2004.
- [14] J. Oliver, S. Oller and Cante, "A plasticity model for simulation of industrial powder compaction processes", *International Journal of Solids and Structures*, 33(20), 3161-3178, 1996.
- [15] D. Perić, M. Vaz and D. R. J. Owen, "On adaptive strategies for large deformations of elasto-plastic solids at finite strains: computational issues and industrial applications", *Computer methods in applied mechanics and engineering*, 176(1), 279-312, 1999.

List of symbols

p_0	Maximum contact pressure	[MPa]
a	Contact length half-width	[mm]
P	Normal load	[N/mm]
E	Elastic modulus	[MPa]
ν	Poisson ratio	[No unit]
μ	Friction coefficient	[No unit]